Supplementary figure

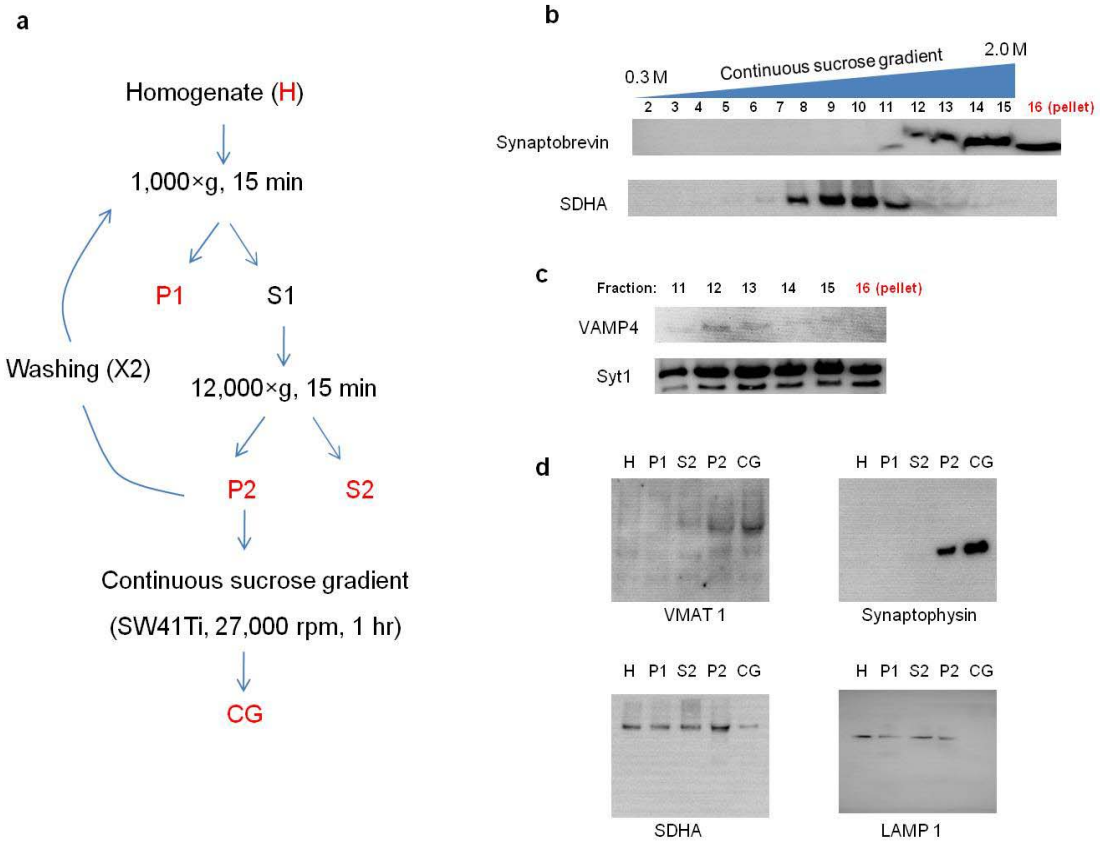

Supplementary figure 1 Purification of CGs from bovine adrenal glands. (**a**) Overview over the protocol for CG purification. After differential centrifugation, CGs were separated from contaminating organelles on a continuous sucrose density gradient (from 0.3 M to 2.0 M). Due to their high protein content, CGs exhibit a buoyant density that is higher than of most other organelles. (**b**) Profile of synaptobrevin (marker for CG membranes) and succinate dehydrogenase complex subunit A (SDHA, marker for mitochondria) across the gradient fractions. Aliquots of equal volume from the each fraction were subjected to SDS-PAGE and immunoblotting. Mitochondria (SDHA) contaminants were mainly present between fraction 7 and 11, whereas CGs (synaptobrevin) were present between fraction 11 and 16. Purified CGs were collected from the pellet (fraction 16, red). (**c**) Distribution of VAMP-4 (marker for immature CGs) and synaptotagmin-1 (present on both immature and mature CGs) across the gradient. Immature CGs were mainly detected in fraction 12 and 13. (**d**) Shown are full-length blots of representative marker proteins.

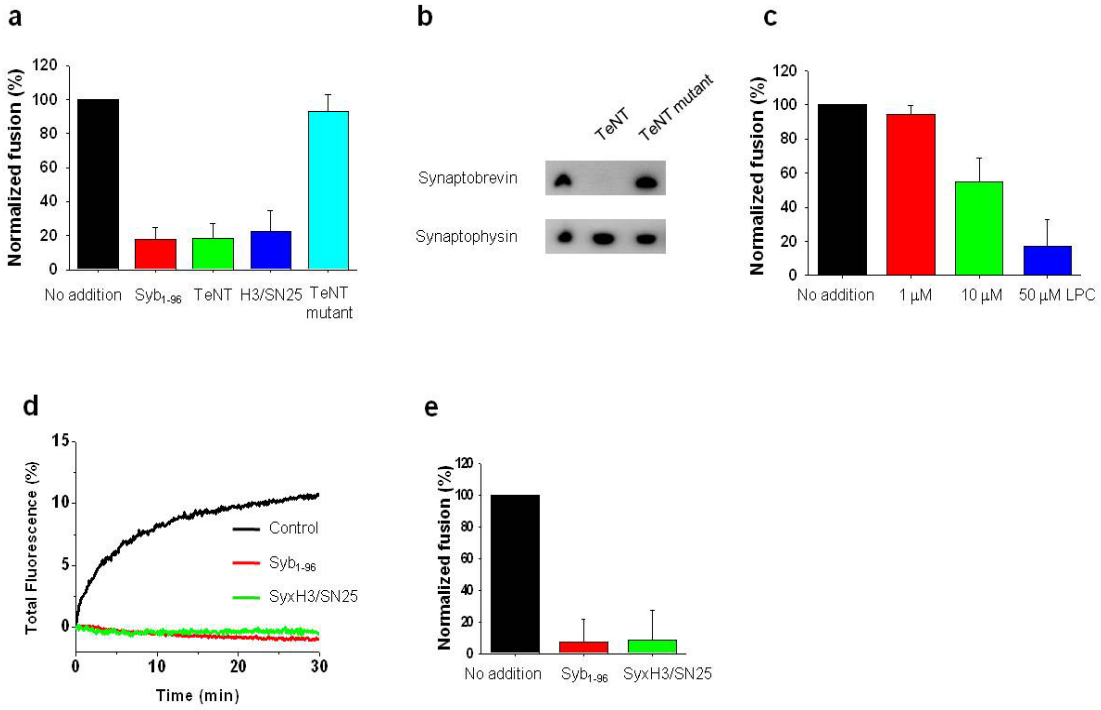

Supplementary figure 2 Characterization of SNARE-dependent fusion of CGs with LUVs containing Q-SNARE complexes. (**a**) Quantification of fusion experiments shown in Figure 1C. All values are normalized to fusion observed under standard conditions. No addition represents basal fusion without any treatment or Ca^{2+}. Data were presented as the percentage of basal fusion reactions after 20 min of reaction time. (**b**) The light chain of tetanus toxin (TeNT) quantitatively cleaves synaptobrevin in CG membranes. CGs were incubated for 30 min at 37°C with 200 nM of purified light chain or a mutant light chain that is inactivated by a point mutation in the Zn^{2+}-coordination site. Synaptophysin served as further control to ensure specificity of toxin action. (**c**) Lysophosphatidylcholine (LPC) inhibits fusion in a dose-dependent manner. (**d**,**e**) SNARE-dependent content mixing using liposomes preloaded with calcein. Dequenching was inhibited by preincubation of the LUVs with soluble Syb_{1-96} and by preincubation of CGs with soluble SyxH3/SN25.

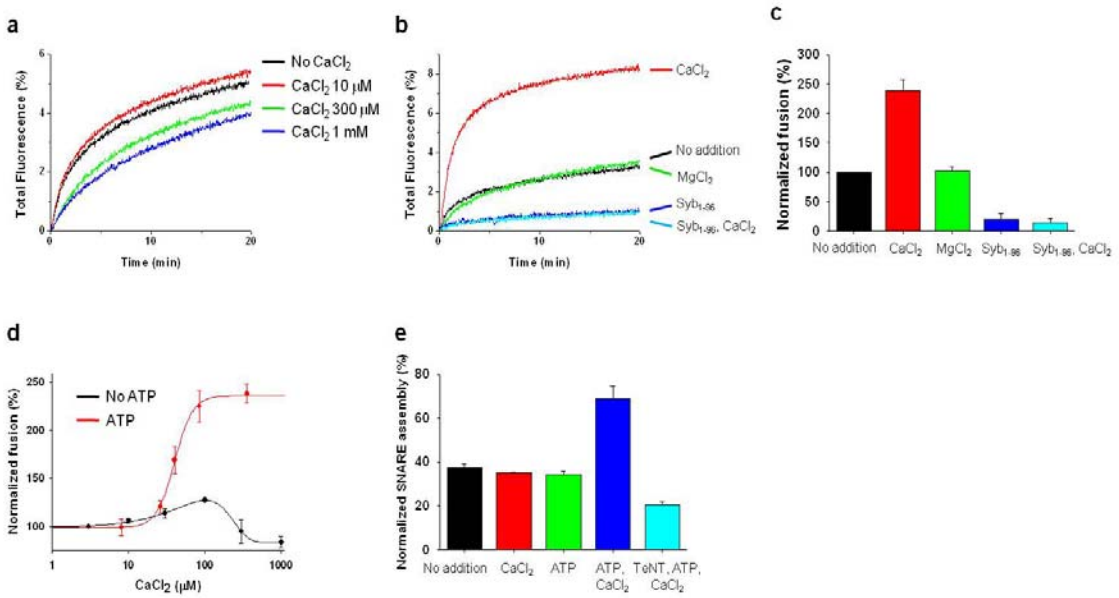

Supplementary figure 3 Influence of Ca^{2+} on SNARE-mediated fusion between CGs and LUVs: further characterization and quantification. (**a**) Dose-dependent inhibition by Ca^{2+} using standard conditions in the absence of ATP. This inhibition resembles that observed previously for purified synaptic vesicles. (**b**,**c**) CG fusion in the presence of ATP (5 mM). 300 µM Ca^{2+} was added resulting in 84 µM of free Ca^{2+} concentration in the presence of 5 mM ATP and enhanced fusion. 300 µM $MgCl_2$ had no effect. Soluble Syb_{1-96} completely blocked fusion regardless of whether Ca^{2+} was present or not. (**d**) Ca^{2+} dose-response curve of CG fusion in the absence and the presence of ATP. Free Ca^{2+} concentration in the presence of ATP was calibrated using the simulation (see Ca^{2+} calibration in the Online Methods). Ca^{2+} was able to accelerate CG fusion only in the presence of ATP (red). (**e**) SNARE assembly was also enhanced by Ca^{2+} in the presence of ATP. Data was presented as the percentage of total SNARE assembly induced by 1 µM unlabeled Syb_{1-96}.

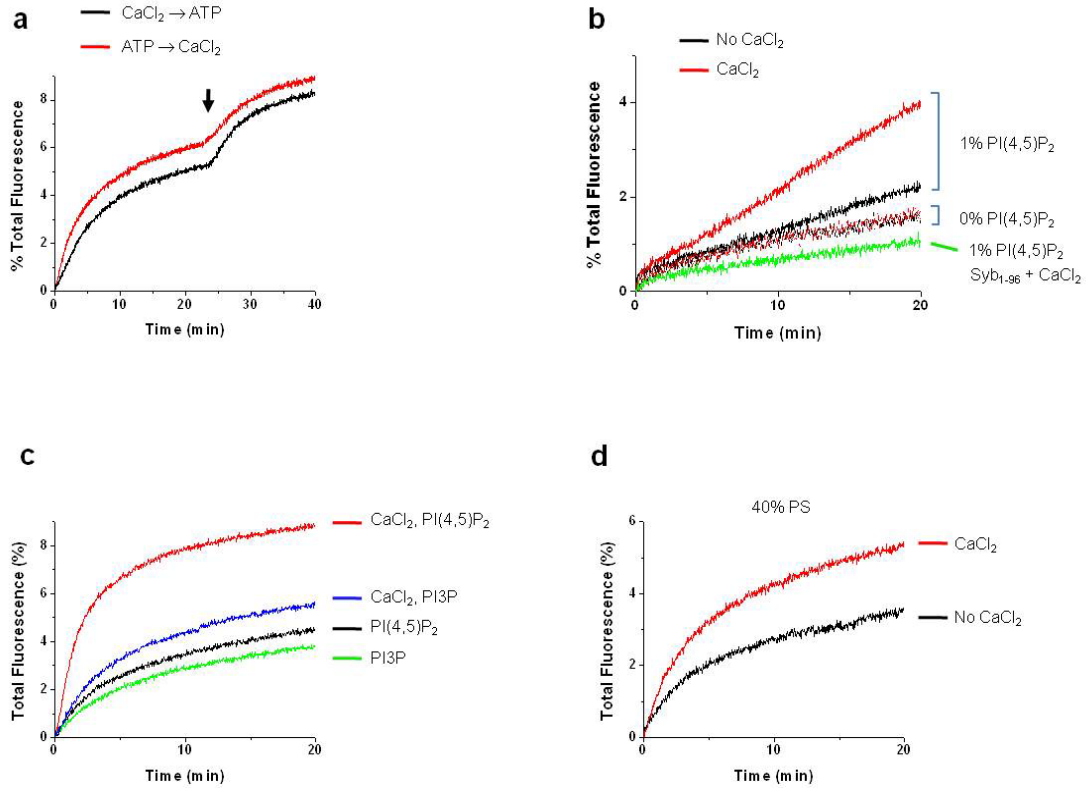

Supplementary figure 4 (**a**) Sequential addition of $CaCl_2$ and ATP caused a step-increase in the fusion reaction upon the 2nd addition, regardless of the order in which $CaCl_2$ and ATP were added. (**b**) Ca^{2+}/ATP-dependent enhancement of fusion is also observable when full length syntaxin-1A and SNAP-25A are used as acceptors in the LUVs. Again, $CaCl_2$ increased CG fusion only in the presence of $PI(4,5)P_2$ in the target membrane (red solid line). Preincubation of $Syb_{1\text{-}96}$ completely abolished Ca^{2+}-induced CG fusion in the presence of $PI(4,5)P_2$ (green line). (**c**) $PI(4,5)P_2$ (1%) in LUVs was replaced by PI3P (1%). (**d**) LUVs contained no phosphoinositides but the PS concentration was increased to 40% (57% PC, 3% labeled PE). 5 mM ATP was added in all of fusion reactions.

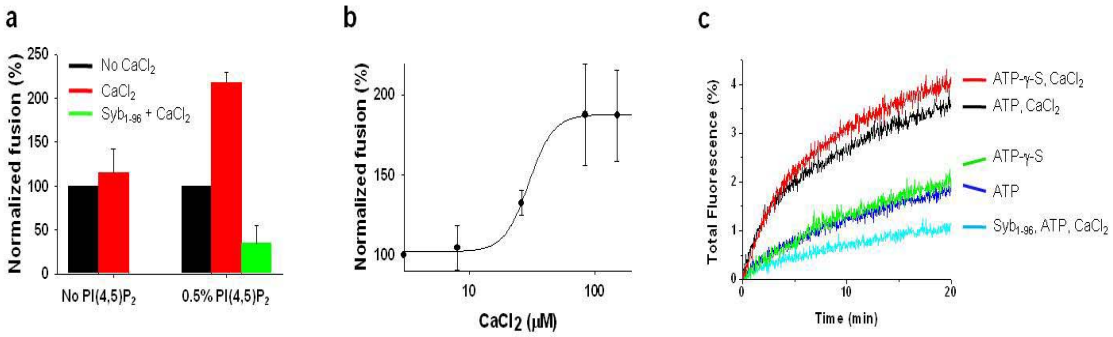

Supplementary figure 5 Ca^{2+}-dependent enhancement of SV fusion does not require ATP hydrolysis but is dependent on $PI(4,5)P_2$ in the target membrane. (**a**,**b**) In the presence of 5 mM ATP, Ca^{2+} (84 μM) increased SV fusion only if the target membrane contains $PI(4,5)P_2$. Soluble synaptobrevin ($Syb_{1\text{-}96}$), an inhibitor of SNARE assembly, blocked Ca^{2+}-dependent SV fusion indicating SNARE-dependent fusion. Dose-response curve of Ca^{2+}-induced SV fusion in the presence of 0.5% $PI(4,5)P_2$ shows EC_{50} of 35.4 ± 3 μM. Fusion was normalized as the percentage of basal fusion without Ca^{2+} after 20 min reaction time. (**c**) Ca^{2+}-dependent enhancement of synaptic vesicle fusion in the presence of ATP also does not require ATP hydrolysis.